






Effect of PCDH19 missense mutations on cell-to-cell proximity and neuronal development under heterotypic conditions

Nami Motosugi ^a, Akiko Sugiyama^a, Asako Otomo ^{a,b,c}, Yuka Sakata^a, Takuma Araki^d, Shinji Hadano ^{a,b,c}, Natsuhiko Kumasaka ^{e,1,*} and Atsushi Fukuda ^{a,b,c,f,*}

^aDivision of Basic Medical Science and Molecular Medicine, Department of Molecular Life Sciences, Tokai University School of Medicine, Isehara, Kanagawa 259-1193, Japan

^bThe Institute of Medical Sciences, Tokai University, Isehara 259-1193, Japan

^cMicro/Nano Technology Center, Tokai University, Hiratsuka, Kanagawa 259-1193, Japan

^dSupport Center for Medical Research and Education, Tokai University School of Medicine, Isehara, Kanagawa 259-1143, Japan

^eGenetics Division, Medical Support Center of the Japan Environment and Children's Study, National Center for Child Health and Development, Tokyo 157-0074, Japan

^fCenter for Regenerative Medicine, National Center for Child Health and Development, Tokyo 157-0074, Japan

¹Present address: Division of Digital Genomics, Human Genome Center, Institute of Medical Science, The University of Tokyo, Tokyo, Japan.

*To whom correspondence should be addressed: Email: kumasaka@hgc.jp (N.K.); Email: fa972942@tsc.u-tokai.ac.jp (A.F.)

Edited By: Marisa Bartolomei

Abstract

The mutation of the X-linked protocadherin (PCDH) 19 gene in heterozygous females causes epilepsy. However, because of the erosion of X-chromosome inactivation (XCI) in female human pluripotent stem cells, precise disease modeling often leads to failure. In this study, using a mathematical approach and induced pluripotent stem cells retaining XCI derived from patients with PCDH19 missense mutations, we found that heterotypic conditions, which are composed of wild-type and missense PCDH19, led to significant cell-to-cell proximity and impaired neuronal differentiation, accompanied by the aberrant accumulation of doublecortin, a microtubule-associated protein. Our findings suggest that ease of adhesion between cells expressing either wild-type or missense PCDH19 might lead to aberrant cell aggregation in early embryonic phases, causing poor neuronal development.

Introduction

A heterozygous mutation of the X-linked protocadherin (PCDH) 19 gene causes monogenic epilepsy in females owing to random X-chromosome inactivation (XCI) (1–3). PCDH proteins are cell-to-cell adhesion molecules related to neurobiological processes such as neurite self-avoidance and synaptogenesis (4, 5). Using an overexpression system of various PCDH classes in K562 cancer cells or model mice with PCDH19 deletion, a recent study demonstrated that the same type of PCDH proteins tended to adhere to each other (1). However, given that the mice with the heterozygous PCDH19 deletion did not exhibit apparent spontaneous seizures (1) and that most patients retained missense mutations (6), the deletion model might not be suitable for understanding PCDH19-related epilepsy.

Although human-induced pluripotent stem cells (hiPSCs) from patients with PCDH19 mutations are beneficial for disease modeling, female hPSCs often cause XCI erosion during culture. XCI erosion causes a dysregulation of X-linked genes, leading to a biallelic expression of X-linked genes (7). Consequently, cells with a heterozygous mutation in the X-linked gene express both wild and

mutant products, thereby preventing proper disease modeling (7, 8). Therefore, XCI must be retained to perform proper ex vivo modeling using female hPSCs. We recently demonstrated that XCI in female hPSCs was maintained with the daily use of the Rho kinase inhibitor, enabling proper disease modeling using female patient-specific iPSCs (8). In this study, using iPSCs derived from PCDH19 missense mutations with XCI (PCDH19^{mut}-iPSCs), we revisited the question of how the PCDH19 missense mutation is linked to neuronal development.

Results

Two iPSC lines from patients with a PCDH19 heterozygous mutation exhibiting epilepsy (PCDH19^{het:mut}-1656 and PCDH19^{het:mut}-2314 lines) were obtained from the RIKEN BioResource Center. An immunofluorescence (IF) analysis using histone 3 lysine 27 trimethylation (H3K27me3), XCI hallmark (9), antibody revealed that 80% of cells in both lines were H3K27me3 foci with the pluripotency marker OCT4 (Fig. S1a and b). These lines retained heterozygous mutations in exon1 of PCDH19, and

Competing interest: The authors declare no competing interest.

Received: March 2, 2023. **Accepted:** January 30, 2024

© The Author(s) 2024. Published by Oxford University Press on behalf of National Academy of Sciences. This is an Open Access article distributed under the terms of the Creative Commons Attribution-NonCommercial-NoDerivs licence (<https://creativecommons.org/licenses/by-nc-nd/4.0/>), which permits non-commercial reproduction and distribution of the work, in any medium, provided the original work is not altered or transformed in any way, and that the work is properly cited. For commercial re-use, please contact reprints@oup.com for reprints and translation rights for reprints. All other permissions can be obtained through our RightsLink service via the Permissions link on the article page on our site—for further information please contact journals.permissions@oup.com.

an expression allele analysis using complementary DNA (cDNA) revealed that PCDH19^{het:mut-1656} and PCDH19^{het:mut-2314} expressed PCDH19 with missense mutations of S139L and V191L, respectively, in a monoallelic manner (Fig. S1c), confirming that these lines were not subjected to XCI erosion.

Given that PCDH19 is an X-linked gene and is subjected to random XCI (1–3), patient cells are in mosaic states, composed of two PCDH19 types (wild type [WT] and mutant). The iPSC clones expressing WT PCDH19 could not be obtained from the same donor with a PCDH heterozygous mutation; therefore, to recapture the in vivo situation (mosaic), mixed cell experiments were conducted using a healthy human embryonic stem cell (hESC) line expressing enhanced green fluorescent protein (EGFP) from the adeno-associated virus integration site safe harbor locus (S6-egfp; Fig. S2). Two other healthy female hPSC lines, adipose-derived stem cell (ADSC)-iPSC and SEES5 (hESC) lines, which retained XCI in >80% of cells, were used as controls in the mixed cell experiments (Healthy-1 and Healthy-2, respectively, Fig. 1a) (8, 10).

To examine whether preferential adhesion occurs in specific cell line pairs, a series of aggregation experiments with various combinations of S6-egfp and other healthy controls or mutant lines were conducted. In the assay, an IF analysis against the GFP antibody was used to distinguish the cell origin and obtain the cell coordinates, followed by a comprehensive evaluation of adhesion status using bespoke mathematical modeling leveraging cell-to-cell proximity (Fig. 1a and Supplementary Methods). The model accounted for the distance distribution of all pairs of cells in the imaging area to classify each pair of cells as either “adhesive” or “nonadhesive” by fitting a bivariate Gaussian mixture model. The latent status of “adhesiveness” was then propagated to logistic regression to jointly and rigorously estimate the odds ratio of cell adhesion between cells from WT and mutant lines over other cell combinations while adjusting the line and donor effects, of which cells from the same donor are proximate, since we did not obtain two cell types expressing either PCDH19 WT or a mutant from the same donor (Fig. S3). Unexpectedly, in contrast to a previous report using PCDH19-deletion mice (1), the model revealed that the odd ratios of cell-to-cell proximity between S6-egfp/mutant pairs over other pairs were significantly higher (Fig. 1b), suggesting that the cells with the missense mutation PCDH19 significantly adhere to those with WT PCDH19.

As PCDH19 is identified as a transmembrane protein (11, 12), we examined whether PCDH19 localization was affected under heterotypic conditions. We first checked the expression levels of PCDH19 mRNA by qPCR in hPSCs used for the aggregation assay. The qPCR analysis revealed that the expression levels of PCDH19 in PCDH19^{mut}-iPSC lines were comparable with those in healthy control lines (Fig. S4a). A western blotting analysis showed that there were no marked differences among the samples (Fig. S4b). The IF analysis showed that PCDH19 was stained in the cell-to-cell border regions, exhibiting a compartment-like staining pattern (Fig. S4c). However, the total percentages of the compartment-like structure per nucleus in WT/PCDH19^{mut} pairs were comparable with those in WT/WT pairs (Fig. S4d). We further examined the expression status of N-cadherin, a potential interactor of PCDH19 (11), by IF. The percentage of N-cadherin particles per nucleus was significantly different in each group, but no specific propensity was observed for the WT/PCDH19^{mut} pairs (Fig. S4e and f). Consequently, although the exact mechanisms underlying the preferential cell-to-cell proximity under PCDH19 heterotypic conditions remain unknown, these results suggest that the expression status of PCDH19 and N-cadherin in iPSCs is not directly linked to the cell-to-cell proximity.

Next, to examine the effect of the PCDH19 missense mutation on neuronal differentiation, cortical neurons were generated under mixed or no-mix culture conditions by the prevalent protocol using small-molecule cocktails (13, 14) (Fig. 2a). We confirmed that the protocol generated the cortical neurons with the expression of a marker, such as T-box brain transcription factor 1 (8) (Fig. S5). On in vitro day (IVD) 40, the neuronal differentiation status was evaluated by an IF analysis using neuronal markers, microtubule-associated protein 2 (MAP2) and metabotropic glutamate receptor 1 (mGLUR1), and EGFP. Interestingly, a significant impairment of neuronal differentiation was observed in PCDH19^{mut}-iPSCs compared with that in healthy controls when the cells were differentiated under the no-mix culture condition (Fig. 2b and c). In the mixed culture condition with S6-egfp, similar to the results from the experiments of the no-mix culture condition, we found that PCDH19^{het:mut}-iPSCs exhibited poor differentiation rates compared with those of healthy controls (ADSC: 97.8%, SEES5: 48.1%, PC-1656: 5.9%, and PC-2314: 24.7% on average; Fig. 2d and e). Moreover, under the mixed culture condition, the Healthy-2 cell line showed decreased differentiation. The exact mechanism for the decreased differentiation of the Healthy-2 lineage is not yet known; one possibility may be that the differentiation timing between the two lines is not synchronized. However, this decrease was more severe in the PCDH19^{het:mut}-iPSC lines, specifically in the PCDH19^{het:mut-1656} line (the ratios of mix/no-mix are as follows: Healthy-1: 1.00-fold, Healthy-2: 0.51-fold, PCDH19^{het:mut-1656}: 0.08-fold, PCDH19^{het:mut-2314}: 0.31-fold; Fig. 2c and e). We further assessed the effect of the PCDH19 missense mutation on neuronal complexity under the mixed culture condition. A Sholl analysis revealed that the neurons derived from PCDH19^{mut}-iPSCs showed a tendency toward poor development compared with those from healthy controls (Fig. S6a and b). The IF analysis of PCDH19 and N-cadherin in neurons showed that both spread in the entire regions of the neurons, but we did not observe the aberrant staining patterns specific to PCDH19 mutant cells (Fig. S7). These results suggest that the neuronal differentiation and complexity of PCDH19^{mut}-iPSCs might be more affected when the cells are cultured under PCDH19 heterotypic conditions without a dramatic alteration of PCDH19 and N-cadherin expression status.

We also examined whether Ca signals were observed in the neurons. Time-lapse imaging using a Ca indicator showed Ca activity in the neurons in both mix and no-mix conditions (Fig. S8), suggesting that the heterotypic conditions did not prevent the generation of Ca signals in the neurons.

The mixed culture experiments using S6-egfp provide an opportunity to examine the effect of heterotypic conditions on the cells with WT PCDH19. Moreover, focusing on the S6-egfp line would eliminate the genetic background effect on differentiation status. Interestingly, the IF analysis of the cells with EGFP⁺ revealed that the differentiation of S6-egfp neurons cultured with the PCDH19 mutant cells was significantly decreased compared with that in healthy controls (Fig. 2f and g). During Sholl analysis, we observed a significant decrease in the complexity of the S6-egfp cell line with PCDH19^{het:mut-1656} (Fig. S6c), whereas the complexity of the S6-egfp cell line with PCDH19^{het:mut-2314} was comparable with that of the healthy cell lines, suggesting that the neuronal complexity of WT cells might be considerably affected by the type of PCDH19 mutation (Fig. S6c).

Next, to examine the developmental status of differentiating cells in the mixed culture conditions, we conducted doublecortin (DCX; immature neuron marker) (15) and SOX2 (progenitor marker) (16) staining at IVD 40 (Fig. S9a). The IF analysis revealed that

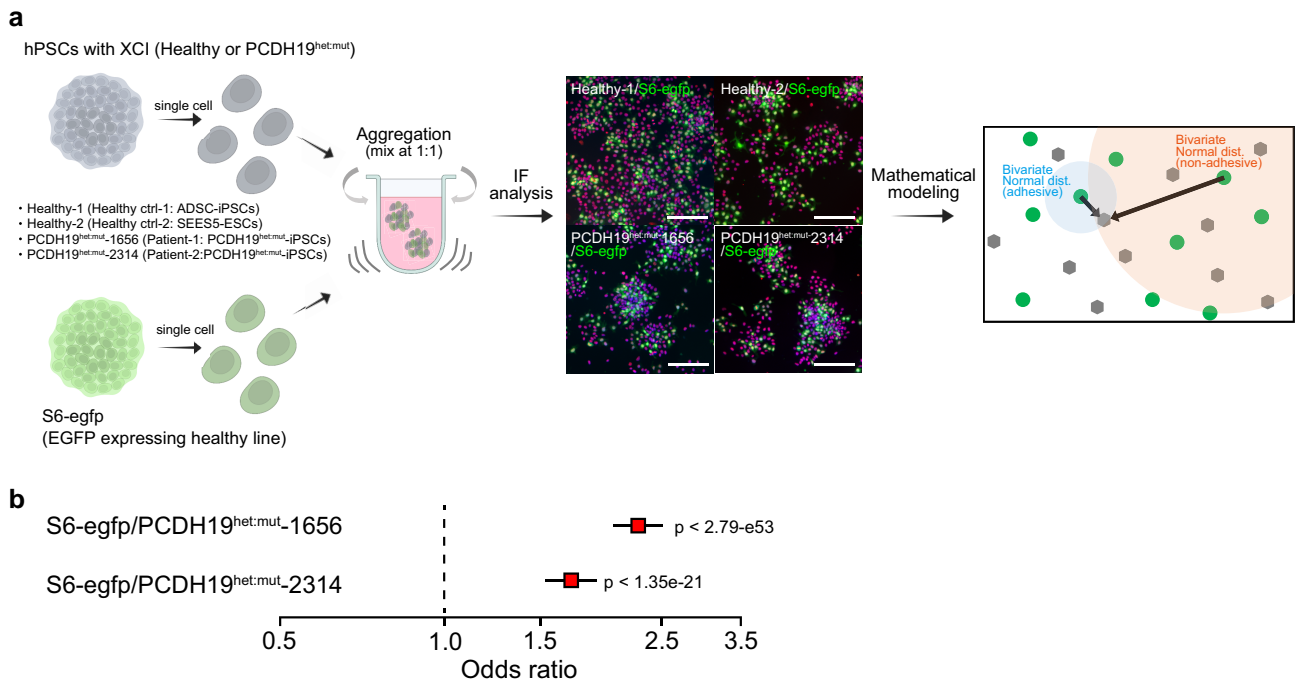


Fig. 1. A PCDH19 heterotypic condition significantly shows cell-to-cell proximity. **a**) An experimental scheme for mathematical modeling of cell adhesion via an aggregation assay. Single cells of S6-egfp line were mixed with another line (healthy ctrl lines: ADSC-iPSC and SEES5, PCDH19^{het:mut}-iPSC lines: PCDH19^{het:mut}-1656 and PCDH19^{het:mut}-2314) at a 1:1 ratio. The mixed cells were subjected to aggregation assay and IF analysis using the OCT4 (red: pluripotency marker) and GFP antibodies. The nuclei were stained with DAPI (blue). The coordinates of each cell were measured in QuPath software, and the mathematical modeling for cell adhesion assay was performed as follows: the schematic shows the distance between two cells, which is modeled by a mixture of two bivariate normal distributions, one for an adhesive pair of cells with smaller variance (proximal) and the other for two random cells (nonadhesive) with larger variance (distal). **b**) Odds ratio of the pair of S6-egfp and PCDH19^{het:mut}-iPSCs. The forest plot shows the estimated odds ratios (effect sizes of the logistic regression model) of heterotypic conditions for the pair of S6-egfp and the two mutant lines over other pairs of lines (see [Supplementary Methods](#) for more details).

the number of SOX2-positive cells in all groups was small (<2% of DAPI; Fig. S9b and c), indicating that the poor differentiation observed in the PCDH19 mutant groups was not caused by the arrest of progenitor phases. In the DCX staining analysis, the population of DCX-positive cells depended on the genetic background (Fig. S9d and e). However, an aberrant DCX staining pattern (foci) was observed in many cells in the PCDH19^{het:mut}-1656/2314 groups (Fig. S8c and d). Specifically, most cells in the PCDH19^{het:mut}-1656/S6-egfp groups, which exhibited a higher cell-to-cell proximity (Fig. 1b), displayed a foci staining pattern, whereas the healthy control lines exhibited the typical staining pattern (spreading in the cytoplasm; Fig. S8c and d). These results suggest that PCDH19 mutations may hinder neuronal maturation phases.

To investigate whether DCX aberrant foci were specifically observed in the PCDH19 heterotypic culture condition and/or in PCDH19 mutant cells, we conducted DCX staining in the no-mix condition of PCDH19^{het:mut}-1656 and PCDH19^{het:mut}-2314 mutants individually. The aberrant foci staining pattern was not observed in most cells in the PCDH19^{het:mut}-1656/2314 groups; rather, these cells exhibited a spreading DCX pattern (Fig. S9f and g). These results indicate that the poor differentiation of PCDH19^{het:mut} mutants in the heterotypic condition is accompanied by aberrant DCX accumulation during neuronal maturation phases.

Finally, to gain insights into the effect of PCDH19 mutations on potential structural changes, we conducted a computational simulation of protein-protein interaction. Given that PCDH19 interacts with other PCDH-family proteins (1), we first assessed the types of PCDH-family proteins expressed in hPSCs using a published RNA-sequencing dataset. PCDH1/10/17/18, in addition to PCDH19, was detected in the two healthy lines (Fig. S10a).

ChimeraX analysis (17), using the predicted 3D structure by AlphaFold2 (18), revealed that the rmsds among PCDH-family proteins (19), including WT PCDH19, were <1.2, suggesting a potential similarity between mutant and PCDH-family proteins (Fig. S10b). The analysis further indicated that the rmsd between PCDH19 and PCDH19^{het:mut}-1656 was 0.684 and that between PCDH19 and PCDH19^{het:mut}-2314 was 0.769 (Fig. S10b). These results suggest that 3D structure of the PCDH19 mutations (S139L: PCDH19^{het:mut}-1656 and V191L: PCDH19^{het:mut}-2314) may not undergo significant changes and that such similarities may be one of the factors responsible for cell-to-cell adhesion.

Overall, the study results demonstrated that the missense mutation PCDH19 was more significantly proximate to normal cells, inducing poor neuronal differentiation accompanied by aberrant DCX accumulation in both wild and mutant cells (Fig. 2h). These results suggest a new possibility for the cause of PCDH19 epilepsy.

Discussion

Given that some patients with PCDH19 epilepsy retain the PCDH19 deletion, the mechanism by which the same class of PCDH19 is clustered might be underlying in such patients, as previously conceived by cancer cells and mice models (1, 11). However, using patient-specific iPSCs with normal XCI, we demonstrated that two different PCDH19 mutant cells shared a similar propensity to adhere to WT cells, inducing poor neuronal development.

With regard to the impaired neuronal differentiation in the heterotypic conditions, we observed an aberrant accumulation of DCX (Fig. S9). Given that DCX is an X-linked gene and that heterozygous mutations can cause subcortical band heterotopia, which

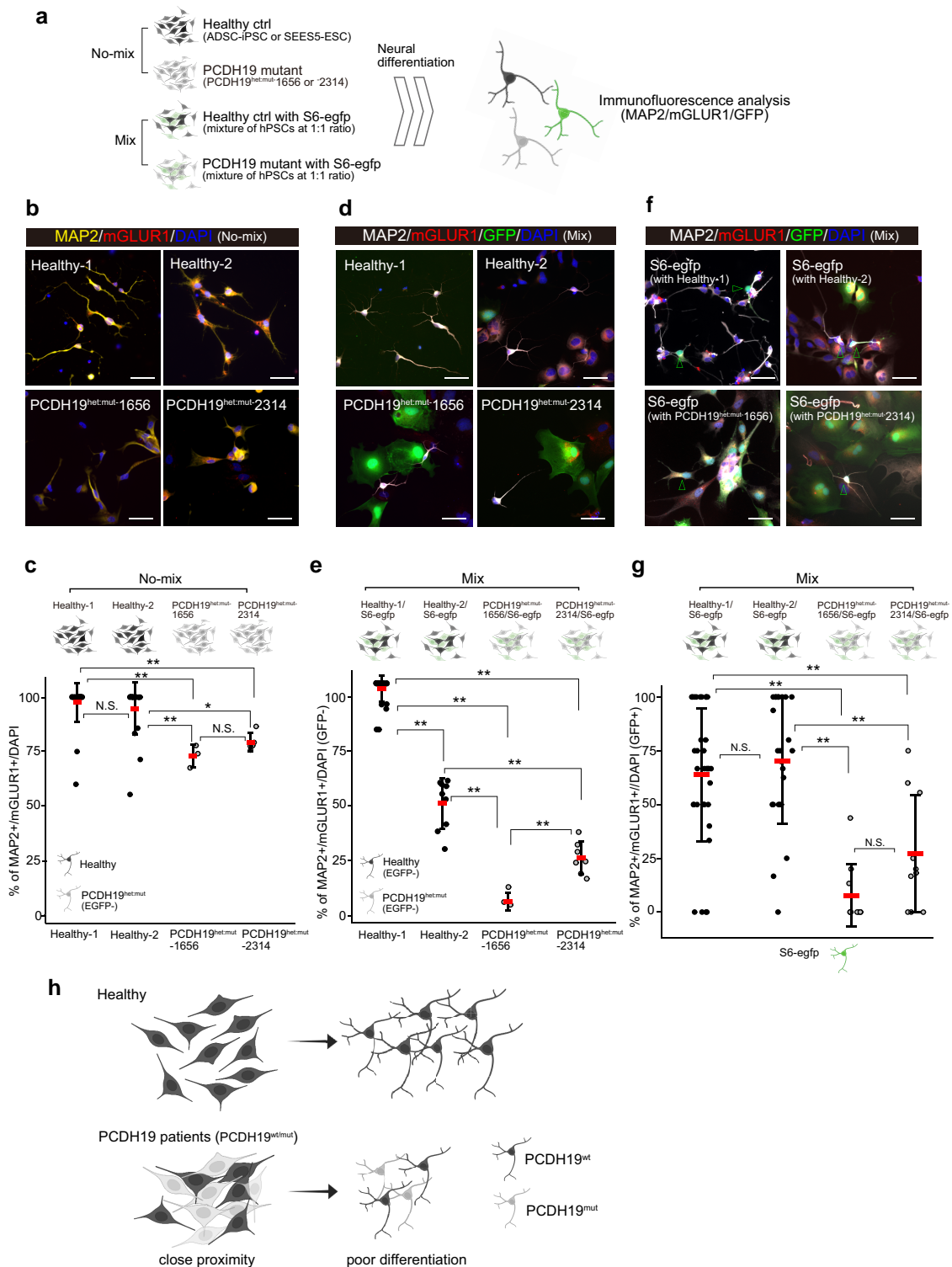


Fig. 2. The heterotypic condition of PCDH19 impairs neuronal differentiation. **a**) An experimental scheme for the assay of neuronal differentiation under PCDH19 heterotypic conditions. Differentiation into cortical neurons from hPSCs was performed in either single or mixed cell line conditions. In the mixed culture experiments, an hPSC line was cocultured with S6-egfp WT at the same cell number (1:1 ratio) and differentiated into neurons. An IF analysis was used to evaluate the differentiation status. Anti-GFP was used to distinguish the cell origins. **b** and **c**) Neuronal differentiation in a single cell line culture. The representative images (**b**) and the quantification results of MAP2⁺/mGLUR1⁺ cells are shown (**c**). **d** and **e**) Neuronal differentiation in mixed culture. The representative images (**d**) and the quantification results of MAP2⁺/mGLUR1⁺/GFP⁻ cells are shown (**e**). **f** and **g**) Neuronal differentiation in mixed culture. The representative images (**f**) and the quantification results of MAP2⁺/mGLUR1⁺/GFP⁺ cells are shown (**g**). The arrowheads indicate the neuron from the S6-egfp line. Each dot represents the percentage of positive cells from an individual imaging area. At least 99 neurons were analyzed in each experimental group. One-way ANOVA with a post hoc test (Tukey) was applied to multiple comparisons. **h**) A model for PCDH19 epilepsy onset. Owing to random XCI, the cells with the PCDH19 missense mutation expressed either missense or WT PCDH19. Consequently, the heterotypic conditions generated more cell-adhesive situations. The proximity between cells induced poor neural differentiation, which might be the cause of PCDH19 epilepsy.

can lead to epilepsy and is predominantly observed in females (20), a PCDH19-related disorder might be partially linked to the abnormal accumulation of DCX. In addition to the marked accumulation of DCX observed in the PCDH19^{het:mut}-1656 group (Fig. S9d and e), this group also exhibited more pronounced deficiencies in neuronal differentiation (Fig. 2e and g), complexity (Fig. S6b and c), and high cell-to-cell proximity (Fig. 1b), compared with the PCDH19^{het:mut}-2314 group. These results suggest that the more proximal cells are to each other, the worse the neuronal differentiation.

We further observed that the influence of neuronal complexity between WT and mutant cells was different in the PCDH19^{het:mut}-2314/s6-egfp pair (Fig. S6b and c). Given that a part of PCDH19 associates with chromatin remodeler neuroLSD1, affecting gene expression related to differentiation, memory, and cognitive functions (21, 22), the finding suggests that the gene expression status related to neural complexity may be more affected in mutant cells than in WT cells and/or by the type of mutation.

The detailed molecular mechanisms underlying the preferential adhesion and impairment of neuronal development under PCDH19 heterotypic conditions are yet to be fully elucidated. However, considering that there are ~500 X-linked genes, including PCDH19 and DCX, associated with diseases (23), the disease modeling using patient-specific iPSCs retaining XCI could be beneficial to elucidate precise disease mechanisms in females.

Acknowledgments

The authors thank the members of the Support Center for Medical Research and Education, Tokai University School of Medicine, for assisting with various experiments. Some figures were prepared using BioRender.

Supplementary Material

[Supplementary material](#) is available at PNAS Nexus online.

Funding

This study was supported by AMED (Japan Agency for Medical Research and Development) under grant number 22bm0804030h0002 to A.F.

Author Contributions

N.M., N.K., and A.F. conceptualized and designed the study; N.M., A.S., A.O., T.A., and Y.S. conducted cellular and molecular biology experiments; N.M., A.S., A.O., Y.S., S.H., N.K., and A.F. analyzed the data; N.K. performed the mathematical modeling and data analysis; N.M., N.K., and A.F. wrote the manuscript with input from all the authors; and N.K. and A.F. supervised the study.

Data Availability

All study data are included in the article and [supplementary material](#).

References

- Pederick DT, et al. 2018. Abnormal cell sorting underlies the unique X-linked inheritance of PCDH19 epilepsy. *Neuron*. 97:59–66.e5.
- Dibbens LM, et al. 2008. X-linked protocadherin 19 mutations cause female-limited epilepsy and cognitive impairment. *Nat Genet*. 40:776–781.
- Depienne C, et al. 2009. Sporadic infantile epileptic encephalopathy caused by mutations in PCDH19 resembles Dravet syndrome but mainly affects females. *PLoS Genet*. 5:e1000381.
- Lefebvre JL, Kostadinov D, Chen WV, Maniatis T, Sanes JR. 2012. Protocadherins mediate dendritic self-avoidance in the mammalian nervous system. *Nature*. 488:517–521.
- Hayashi S, Takeichi M. 2015. Emerging roles of protocadherins: from self-avoidance to enhancement of motility. *J Cell Sci*. 128:1455–1464.
- Niazi R, Fanning EA, Depienne C, Sarmady M, Abou Tayoun AN. 2019. A mutation update for the PCDH19 gene causing early-onset epilepsy in females with an unusual expression pattern. *Hum Mutat*. 40:243–257.
- Mekhoubad S, et al. 2012. Erosion of dosage compensation impacts human iPSC disease modeling. *Cell Stem Cell*. 10:595–609.
- Motosugi N, et al. 2022. De-erosion of X chromosome dosage compensation by the editing of XIST regulatory regions restores the differentiation potential in hPSCs. *Cell Rep Methods*. 2:100352.
- Motosugi N, et al. 2021. Deletion of lncRNA XACT does not change expression dosage of X-linked genes, but affects differentiation potential in hPSCs. *Cell Rep*. 35:109222.
- Fukuda A, et al. 2021. De novo DNA methyltransferases DNMT3A and DNMT3B are essential for XIST silencing for erosion of dosage compensation in pluripotent stem cells. *Stem Cell Reports*. 16:2138–2148.
- Hoshina N, Johnson-Venkatesh EM, Hoshina M, Umemori H. 2021. Female-specific synaptic dysfunction and cognitive impairment in a mouse model of PCDH19 disorder. *Science*. 372:eaaz3893.
- Kahr I, Vandepoele K, van Roy F. 2013. Delta-protocadherins in health and disease. *Prog Mol Biol Transl Sci*. 116:169–192.
- Xiang Y, et al. 2020. Dysregulation of BRD4 function underlies the functional abnormalities of MeCP2 mutant neurons. *Mol Cell*. 79:84–98.e9.
- Shi Y, Kirwan P, Livesey FJ. 2012. Directed differentiation of human pluripotent stem cells to cerebral cortex neurons and neural networks. *Nat Protoc*. 7:1836–1846.
- Francis F, et al. 1999. Doublecortin is a developmentally regulated, microtubule-associated protein expressed in migrating and differentiating neurons. *Neuron*. 23:247–256.
- Amador-Arjona A, et al. 2015. SOX2 primes the epigenetic landscape in neural precursors enabling proper gene activation during hippocampal neurogenesis. *Proc Natl Acad Sci U S A*. 112:E1936–E1945.
- Pettersen EF, et al. 2021. UCSF chimerax: structure visualization for researchers, educators, and developers. *Protein Sci*. 30:70–82.
- Terwilliger TC, et al. 2022. Improved AlphaFold modeling with implicit experimental information. *Nat Methods*. 19:1376–1382.
- Carugo O, Pongor S. 2001. A normalized root-mean-square distance for comparing protein three-dimensional structures. *Protein Sci*. 10:1470–1473.
- Moreira I, et al. 2015. Paternal transmission of subcortical band heterotopia through DCX somatic mosaicism. *Seizure*. 25:62–64.
- Gerosa L, et al. 2022. The epilepsy-associated protein PCDH19 undergoes NMDA receptor-dependent proteolytic cleavage and regulates the expression of immediate-early genes. *Cell Rep*. 39:110857.
- Perillo B, Tramontano A, Pezone A, Migliaccio A. 2020. LSD1: more than demethylation of histone lysine residues. *Exp Mol Med*. 52:1936–1947.
- Migeon BR. 2020. X-linked diseases: susceptible females. *Genet Med*. 22:1156–1174.